JET Volume 15 (2022) p.p. 23-50
Issue 1, June 2022
Type of article: 1.01
www.fe.um.si/si/jet.html

THE IMPACT OF UNBALANCED POWER SUPPLY ON LOAD CURRENTS IN TRANSIENT AND STEADY-STATE OPERATION

VPLIV NESIMETRIČNIH NAPAJALNIH NAPETOSTI NA TOKE BREMEN MED USTALJENIM OBRATOVANJEM IN MED PREHODNIMI POJAVI

Nina Štumberger[1], Matej Pintarič[2], Gorazd Štumberger[2ℜ]

Keywords: unbalanced power supply voltages, load currents, steady state, transients, Dommel's method, increase in released heat Abstract

Abstract

The impact of unbalanced power supply voltages on power derating, increases in current values and the heat released from electrical machines and devices is typically analysed in quasi-steady-state operation using sequence components. The ratios between the negative and positive sequence voltage and the homopolar (zero) and positive sequence voltage are used to evaluate the level of voltage unbalance. This paper proposes an extension of this approach that includes subtransient, transient and quasi-steady-state operation of wye (grounded and ungrounded) and delta connected loads, consisting of resistors and magnetically linear and non-linear iron core inductors, which is a novelty. Dommel's method for dynamic simulation of electrical circuits,

ℜ Corresponding author: Professor dr. Gorazd Štumberger, Tel.: +386 (0)2-220-7075, Mailing address: Koroška cesta 46, 2000 Maribor, Slovenia. E-mail address: gorazd.stumberger@um.si, nina.stumberger@rwth-aachen.de

[1] RWTH Aachen University (Rheinisch Westfälische Technische Hochschule), Fakultät für Elektrotechnik und Informationstechnik, Schinkelstr. 2, 52062 Aachen, Germany

[2] University of Maribor, Faculty of Electrical Engineering and Computer Science, Koroška cesta 46, 2000 Maribor, Slovenia

based on the modified nodal potential method, time discretisation and implicit numerical integration, is applied to evaluate the impact of unbalanced power supply voltages on load currents. The magnetically non-linear behaviour of the iron core inductors is accounted for by introducing variable dynamic inductances inside Dommel's method. The integrals of instantaneous values of squared load branch currents values in subtransient, transient and quasi-steady-state operation, determined for different levels of unbalance in supply voltages, are normalised with those calculated for the balanced power supply voltages in quasi-steady-state. The obtained ratios of the integrals are used to implicitly evaluate the impact of unbalance in supply voltages on the increase in released heat due to Joule losses. The proposed approach is generally applicable, while the results are shown for the case study of iron core inductors with magnetically linear and non-linear behaviour.

Povzetek

Vpliv nesimetrije v sinusnih napajalnih napetostih na zmanjšanje moči, povečanje tokov in Joulskih izgub električnih strojev in naprav običajno obravnavamo v kvazi stacionarnih (vnihanih) stanjih, pri tem pa uporabljamo simetrične komponente. Merilo nesimetrije sta najpogosteje razmerji med napetostjo negativnega in pozitivnega ter ničnega in pozitivnega zaporedja simetričnih komponent. To delo predstavlja razširitev opisanega pristopa saj vključuje subrtanzientno, tranzientno in kvazi stacionarno območje delovanja v zvezdo in v trikot vezanih bremen, sestavljenih iz zaporedne vezave upora in tuljave z železnim jedrom z magnetno linearnim in magnetni nelinearnim obnašanjem. To je novost, s katero ta prispevek presega obstoječe pristope. Za ovrednotenje vpliva nesimetrije v sinusnih napajalnih napetostih na toke bremen je uporabljena Dommel-ova metoda dinamične simulacije električnih vezij, ki temelji na modificirani metodi vozliščnih potencialov, implicitni metodi numerične integracije povezane s časovno diskretizacijo. Magnetno nelinearno obnašanje tuljave z železnim jedrom je upoštevano z uporabo spremenljive dinamične induktivnosti, ki je smiselno integrirana v Dommel-ovo metodo. Integrali kvadratov trenutnih vrednosti tokov bremen, so izračunani za subtranzientno, tranzientno in kvazi stacionarno obratovanje in določeni za različne stopnje nesimetrije v sinusnih napajalnih napetostih. Za potrebe primerjave so podeljeni z vrednostmi integralov kvadratov tokov bremen pri napajanju s simetričnimi sinusnimi napetostmi pri kvazi stacionarnem obratovanju. S tem smo dobili normirano obliko, ki implicitno omogoča ovrednotenje vpliva nesimetrije v sinusnih napajalnih napetostih na toploto sproščeno v obliki Joulskih izgub. Predstavljena metoda je splošno uporabna in jo je mogoče generalizirati, njeno delovanje pa je v tem delu predstavljeno na primeru tuljav z železnim jedrom z magnetno linearnim in z magnetno nelinearnim obnašanjem.

1 INTRODUCTON

With a balanced three-phase power supply, the voltages are sinusoidal, of equal amplitude and phase-shifted to each other by 120°. An uneven distribution of loads over the three phases or errors in the electrical network, such as short circuits, other faults and different unexpected operating conditions, can cause voltage unbalances *[1]*. The unbalances in voltage supply are usually treated in quasi-steady-state operation of electrical machines and devices using sequence components – the positive (1), the negative (2) and the homopolar (0) component. The level of supply voltage unbalances is evaluated through the ratios of the negative and the homopolar sequence component with respect to the positive one *[1], [2]*.

The supply voltage unbalances can negatively affect the equipment connected to the power supply due to an increase in line currents. This increase causes an increase in Joule losses, which increases the operating temperature and can cause deterioration of the isolation and negatively affect the lifespan of the equipment *[1]*. Most of the authors of existing research have focused on the impact of supply voltage unbalances on the quasi-steady-state operation of induction machines. The impact of angle unbalance in supply voltages on operational properties of induction machines is investigated in *[3]*. The authors in *[4, 5]* deal with the performance analysis of induction machines supplied with unbalanced sinusoidal voltages in quasi-steady-state operation. The influence of unbalanced sinusoidal and balanced non-sinusoidal supply voltages on the performance of a squirrel-cage induction motor is analysed in *[6]*. The impact of supply voltage unbalances on the precise derating and energy performance of three-phase induction motors is discussed in *[7]* and *[8]* respectively. The modelling effect of supply voltage unbalances in systems with adjustable speed drives is described in *[9]*. The author in *[10]* analyses the influence of supply voltage unbalances, combined with over voltages and under voltages, on induction machine winding temperature and loss of insulation life. In *[11]*, the authors deal with thermal effects in the induction machine stator caused by mechanical overloads and supply voltage unbalances. Calorimetric and finite element simulations are applied in *[12]* to evaluate the impact of supply voltage unbalances on induction motor derating.

Transient operation and magnetically non-linear load behaviour are not considered in any of the aforementioned publications. Although the loads considered in this paper are iron core inductors, the proposed approach is new. It enables the treatment of magnetically linear and non-linear behaviour, including subtransient, transient and quasi-steady-state operation. Using a method similar to the one described in *[13]*, the approach proposed in this paper can be further developed to be suitable for treating iron core inductors and electrical machines.

The aim of this paper is to propose a unified method for evaluating the impact of supply voltage unbalances on the increase in currents and Joule losses of wye and delta connected loads, considering the magnetically linear or non-linear behaviour of the iron core of the load, including subtransient, transient and quasi-steady-state operation.

This paper deals with the impact of supply voltage unbalances on the currents and Joule losses of a three-phase load consisting of iron core inductors connected into the delta, ungrounded and grounded wye. Voltage unbalances of up to 10% are considered. To observe the currents in the transient states as well as in quasi-steady-state operation, the load as well as the supply line are modelled using Dommel's method and simulated in MATLAB. The load model represents iron core inductors with magnetically linear and non-linear behaviour. The iron core saturation is considered by introducing variable dynamic inductance, the value of which decreases when the current reaches a certain threshold. Since the aim of this paper is to explore the effect of supply voltage unbalances on a general load, no specific equipment is considered, although this is an area that could be explored in the future.

The theoretical background for evaluating the supply voltage unbalance and Dommel's method are described in Section 2. Section 3 explains the proposed methodology. The results obtained considering different levels of unbalances in supply voltages in the cases of wye and delta connected iron core inductors with magnetically linear and non-linear behaviour are illustrated in Section 4. In Section 5, the findings are summarised and conclusions are drawn.

2 THEORETICAL BACKGROUND

Subsection 2.1 describes the relations among the phasors of phase voltages and sequence component voltages. The latter are used to introduce two factors for evaluating unbalances in sinusoidal supply voltages. Subsection 2.2 provides a comprehensive description of Dommel's method.

2.1 Voltage unbalances

Whilst the degree of voltage unbalance can be described in multiple ways, this paper uses the definition of the International Electrotechnical Commission (IEC), which can be found in *[2]*. It describes how much negative (2) and zero-sequence (0) voltage is superposed on the positive-sequence (1) voltage. The connection between positive-sequence ($\underline{V}_1$), zero-sequence ($\underline{V}_0$), and negative-sequence ($\underline{V}_2$) voltages and the phase voltages ($\underline{V}_a$, $\underline{V}_b$, $\underline{V}_c$) is described by equation (2.1):

$$\begin{bmatrix} \underline{V}_a \\ \underline{V}_b \\ \underline{V}_c \end{bmatrix} = \begin{bmatrix} 1 & 1 & 1 \\ 1 & a^2 & a \\ 1 & a & a^2 \end{bmatrix} \cdot \begin{bmatrix} \underline{V}_0 \\ \underline{V}_1 \\ \underline{V}_2 \end{bmatrix}, \tag{2.1}$$

where $a = \exp\left(j2\frac{\pi}{3}\right)$ *[4]*.

The voltage unbalance factor (VUF) is defined by the ratio between the negative-sequence and positive sequence voltage, as given by (2.2):

$$\mathrm{VUF} = \frac{V_2}{V_1}. \tag{2.2}$$

Along with the delta and ungrounded wye connection of the load, where zero-sequence voltage unbalance has no effect on the load currents, this paper also deals with the grounded wye connection of the load. Therefore, the zero-sequence voltage unbalance factor (ZSVUF), defined by (2.3):

$$\mathrm{ZSVUF} = \frac{V_0}{V_1} \tag{2.3}$$

is used.

2.2 Dommel's method

In order to analyse the transient-state currents, as well as the quasi-steady-state currents, the inductors representing the loads and the connection lines were modelled using Dommel's method, as described in *[14]*. The basis for this model is the equation for the inductor voltage U_L given by (2.4):

$$u_L(t) = v_k(t) - v_m(t) = L\frac{d\, i_{km}}{dt}, \tag{2.4}$$

from which the equation for the inductor current i_{km}, given in equation (2.5)

$$i_{km}(t) = i_{km}(t\text{-}\Delta t) + \frac{1}{L}\int_{t-\Delta t}^{t} \left(v_k(\,) - v_m(\,)\right) d \tag{2.5}$$

is derived by integration over a time period Δt. *t* is the current point in time, τ is an auxiliary variable, L is the inductance of the inductor while $v_k(t)$ and $v_m(t)$ are the potentials on either end of the inductor, as shown in Figure 1.

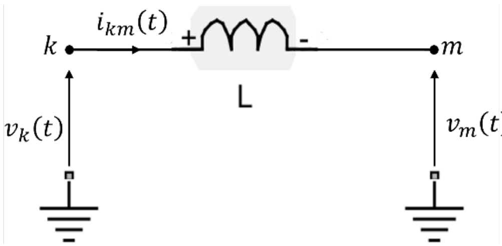

Figure 1: *Inductor with defined potentials and inductor current*

The integral is approximated using the trapezoidal rule, given by (2.6):

$$x(t+\Delta t) = x(t) + \Delta t\,\frac{1}{2}\left(f\left(x(t+\Delta t), t+\Delta t\right) + f\left(x(t), t\right)\right), \tag{2.6}$$

where *f* is the integrated function and *x* is the value of the integral.

When the trapezoidal rule (2.6) is applied to (2.5) and the potentials are grouped according to the points in time (t, t-Δt), equation (2.7) is obtained.

$$i_{km}(t) = i_{km}(t\text{-}\Delta t) + \frac{\Delta t}{2L}\left(v_k(t\text{-}\Delta t) - v_m(t\text{-}\Delta t)\right) + \frac{\Delta t}{2L}\left(v_k(t) - v_m(t)\right) \tag{2.7}$$

It is evident that the inductor current at a given time depends on the inductor current and potential difference over the inductor in the previous time step, and the potential difference over the inductor in the current time step. $\frac{2L}{\Delta t}$ is a constant and represents the effective resistance of the inductor. The terms describing the conditions in the previous time step can be summarised into the current, $I_{km}(t\text{-}\Delta t)$ which describes the history of the inductor current. Thus, equation (2.7) can be rewritten as equation (2.8)

$$i_{km}(t) = I_{km}(t\text{-}\Delta t) + \frac{\Delta t}{2L}\left(v_k(t) - v_m(t)\right), \tag{2.8}$$

and the inductor can be modelled as a current source connected in parallel with the effective resistance, as can be seen in the circuit shown in Figure 2.

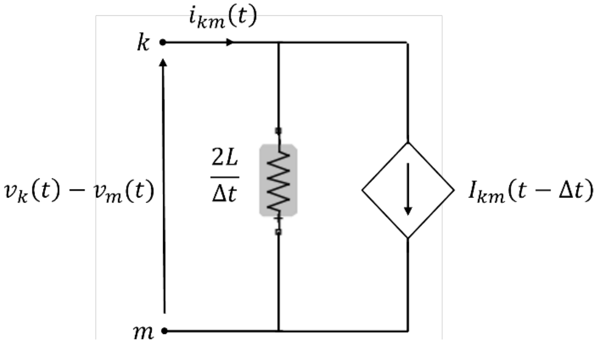

Figure 2: *Model of an inductor according to Dommel's method*

3 PROPOSED METHOD

In this section, the circuit models for the different types of load connections are shown. Furthermore, the types and degrees of supply voltage unbalance used in the simulation are described, together with the approach used to consider the magnetically non-linear behaviour of the iron core inductor.

3.1 Circuit models

The circuit model consists of the power supply and connection line, which are the same for all types of load connection, and the load consisting of iron core inductors, which was connected in either delta, ungrounded or grounded wye. The power supply is modelled as a real current source in each of the phases, as can be seen in Figure 3, where the current of a phase $i_j(t)$ is defined by equation (3.1)

$$i_n(t)=\frac{1}{R}u_n(t), \tag{3.1}$$

where R is the inner resistance of the current source, which is chosen to be 10mΩ. $u_j(t)$ is the supply voltage of that phase and n denotes one of the phases, namely '*a*', '*b*', or '*c*', n {a,b,c}. The supply voltage is sinusoidal with a frequency of 50Hz and is defined by (3.2):

$$u_n(t)=\mathrm{Re}\left\{\sqrt{2}\ \underline{V}_n\ \exp\left(j\ 2\ \pi\ 50\ t\right)\right\}, \tag{3.2}$$

where $\underline{V}_n$ denotes the phasor of a phase voltage defined by (2.1). The voltage source is transformed into a current source to enable nodal potential analysis, which is used to calculate the line currents in transient and quasi-steady-state operation.

The connection line supplying the load in each phase is modelled as an inductor, in accordance with Dommel's method, in series with a resistor, as shown in Figure 3. The chosen inductance *L* of the connection line is 0.2µH. The resistance of the connection line *R* is chosen to equal the internal resistance of the current source, namely 10mΩ.

Similarly to the connection line, the load in the form of iron core inductors is also modelled as an RL-combination connected in series for each phase of the load in the case of a wye connection, and each load branch in the case of a delta connection. The iron core inductors are modelled according to Dommel's method as either iron core inductors with magnetically linear behaviour, where the inductance is constant, or iron core inductor with magnetically non-linear behaviour, where iron core saturation is considered by variable dynamic inductance. The discussed circuit models are shown in Figures 3 a) to 3 c). The time Δt interval equals 1µs. The chosen inductances of the iron core inductors L_n, where *n* stands for one of the load phases or branches, n {a,b,c}, are 0.233H. The distinction between the load inductances enables the modelling of the iron core inductors with magnetically non-linear behaviour, which is described in subsection 3.3. The load resistance R_L is equal in all branches of the load with a value of 2.08Ω.

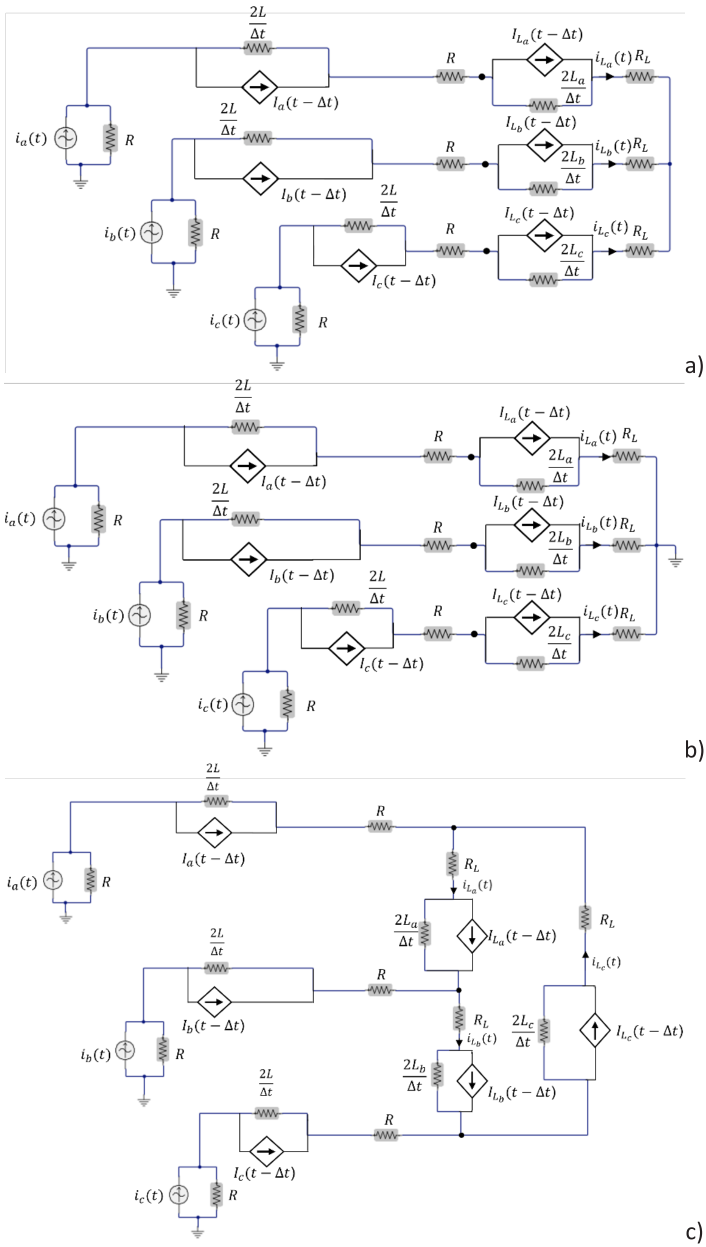

Figure 3: *Circuits models with the three-phase loads a) ungrounded wye connected, b) grounded wye connected and c) delta connected*

To perform the nodal potential analysis, the current vector *I* and the admittance matrix *G* are determined based on the circuit models. The matrix *G'*, which is inverse of *G*, is then calculated. Using (3.3)

$$V = G' \, I, \tag{3.3}$$

the node potential vector *V* is determined. Based on this vector, the load currents $i_{L_n}(t)$ are determined using equation (2.8). To evaluate the Joule losses, the calculated instantaneous current values are recorded for 0.5s in 1μs time intervals Δt. This time interval is divided into three regions: the first is the subtransient region with a duration of 0.1s, the next is the transient region with a duration of 0.3s, and the last is the quasi-steady-state region with a duration of 0.1s. Within each of these regions, the sum of the squared instantaneous values of the load current is calculated using (3.4)

$$i_{n,sum}^2 = \sum_{k=0}^{\frac{t_{start} - t_{stop}}{\Delta t}} i_{L_n}^2\left(t_{start} + k\Delta t\right). \tag{3.4}$$

To better compare these values in different regions, a sum of squared current values normalised over one period $i_{n,sum,rel}^2$ is calculated for all the discussed regions using (3.4) and (3.5):

$$i_{n,sum,rel}^2 = \frac{i_{n,sum}^2}{N^* i_{n,sum,0}^2}, \tag{3.5}$$

Where *N* is the number of periods in the region of observation, while $i_{n,sum,0}^2$ is the sum of the squared instantaneous current values over one period (20ms) in the quasi-steady-state operation determined for balanced power supply.

Since the Joule losses of the load are proportional to the sum of the squared instantaneous values of the load currents, the normalised sum (3.5) represents the increase of Joule losses over one period compared to those over one period (20ms) in normal quasi-steady-state operation of the load supplied with balanced sinusoidal voltages.

3.2 Unbalanced power supply

The negative-sequence and zero-sequence voltage unbalance factors are used to evaluate the level of voltage unbalance. The negative-sequence voltage unbalance factor VUF (2.2) is applied to all three types of load connection, with the VUF ranging from 0 to 10% in 2% intervals. The zero-sequence voltage unbalance factor ZSVUF (2.3) is only applied to the circuit with grounded wye connected load, since it has no effect on the currents of ungrounded wye and delta connected loads. The ZSVUF, defined by (2.3), is increased from 0 to 10% in 2% steps. Additionally, the effect of equal negative-sequence and zero-sequence voltage unbalance simultaneously is investigated for the grounded wye connected load. Figure 4 shows the three-phase supply voltages: the balanced (Figure 4 a)), those with a 10% VUF (Figure 4 b)), those with a 10% ZSVUF (Figure 4 c)), and those with a 10% VUF and a 10% ZSVUF (Figure 4 d)).

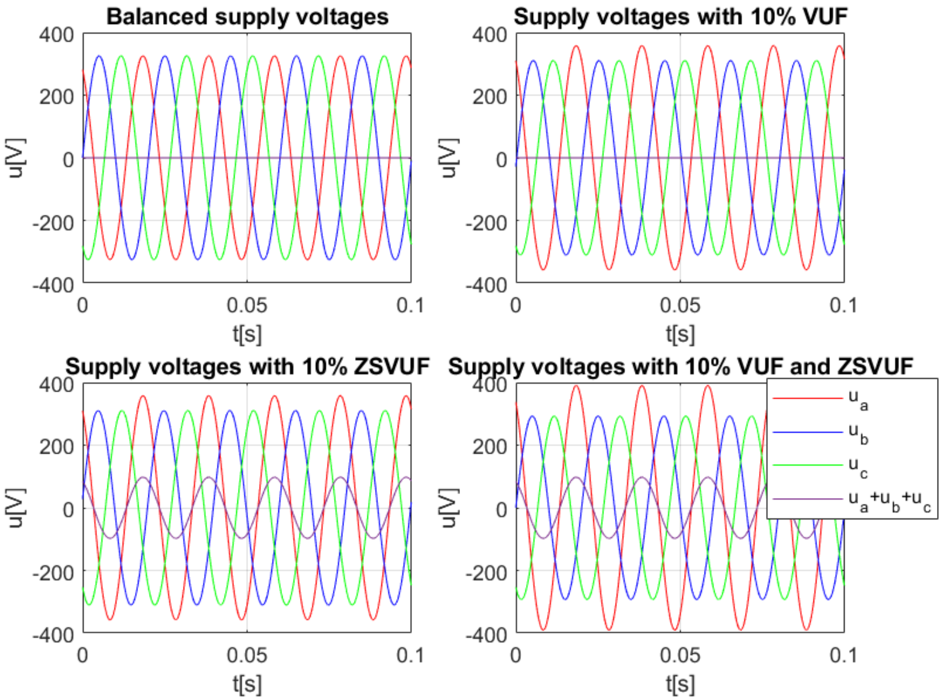

Figure 4: *Supply voltages* u_a, u_b, u_c *and* $u_a + u_b + u_c$ *over time for a) balanced power supply, b) 10% VUF, c) 10% ZSVUF, d) 10% VUF and ZSVUF*

3.3 Iron core saturation

To model a load consisting of iron core inductors with magnetically non-linear behaviour, the current dependent dynamic inductance L_d *[15]* is introduced (3.6):

$$u = \frac{d\Psi(i)}{dt} = \frac{\partial \Psi(i)}{\partial i}\frac{di}{dt} = L_d(i)\frac{di}{dt}, \tag{3.6}$$

where Ψ is the flux linkage, u is the voltage over the iron core inductor, and i the current through the iron core inductor.

In the case of an iron core inductor with magnetically linear behaviour, where iron core saturation does not occur, the load inductance is constant for all currents, with the value L_n= 0.233H. In the case of an iron core inductor with magnetically non-linear behaviour, the dynamic inductance decreases when the absolute value of the current through the inductor exceeds the threshold. It is set to 4.5A, which is the amplitude of the load currents in quasi-steady-state operation when supplied with balanced sinusoidal supply voltages. The saturated dynamic inductance is 10 times smaller than the unsaturated one, and has the value L_{dn}= 0.0233H. In each step of the simulation, the dynamic inductances of all iron core inductors in the load are adjusted according to the absolute values of the current flowing through them. The inductors used to model the connection lines behave magnetically linearly and have constant values of inductances.

The iron core inductors with magnetically non-linear behaviour, representing the load, are only used for the cases of delta and grounded wye connected loads. In the case of an ungrounded wye connected load, convergency issues might appear, which would require further investigation.

4 RESULTS

This section illustrates the results of the simulation. Section 4.1 contains the results for a load containing iron core inductors with magnetically linear behaviour, meaning no saturation effects are considered. Section 4.2 shows the results for a load containing iron core inductors with magnetically non-linear behaviour, meaning saturation effects are considered. All the results are shown in two ways. The first is shown using a graph illustrating the time behaviour of the current in the case of a balanced power supply voltage, and the worst case, meaning the case with the highest voltage unbalance for the discussed case. The second is shown using tables that illustrate the values of the sums of the squared instantaneous current values normalised over one period (3.5) as described in subsection 3.1. They represent an increase in per period Joule losses due to the voltage supply unbalances relative to the per period Joule losses in quasi-steady-state operation in the case of symmetrical supply voltages.

4.1 Effects of supply voltage unbalances on iron core inductor loads with magnetically linear behaviour

The simulation was initially conducted for the loads consisting of iron core inductors with magnetically linear behaviour, meaning the inductance in each branch of the load was constant.

Figures 5 shows the current over time in each of the load branches for a balanced voltage supply and a supply with a 10% VUF, and the load connected in ungrounded wye. Figures 6 and 7 show the load currents for a grounded wye and delta connected load.

As can be seen in Figures 5 and 6, in the cases of a grounded or ungrounded wye connected load, the negative-sequence voltage unbalance causes an increase in amplitude of the current in phase ‘*a*’, compared to operation with a balanced power supply, while the currents in phases ‘*b*’ and ‘*c*’ decrease. In the cases of a delta connected load, as seen in Figure 7, the amplitude of the current increases in phases ‘*a*’ and ‘*c*’, and decreases in phase ‘*b*’.

To better illustrate the change in the current time behaviour and its influence on the normalised per period increase in Joule losses, caused by supply voltage unbalances, the level of which is defined by the value of VUF (2.2), the normalised sums of squared instantaneous current values $i^2_{n,sum,rel}$ (3.5) are used. The values of $i^2_{n,sum,rel}$ in load branches are given in Tables 1 to 3 for all three types of load connection, considering different values of the VUF in the subtransient, transient and quasi-steady-state region of operation. The results shown are completed by the sum of $i^2_{n,sum,rel}$ in all three load branches, which represents the total Joule losses in the load.

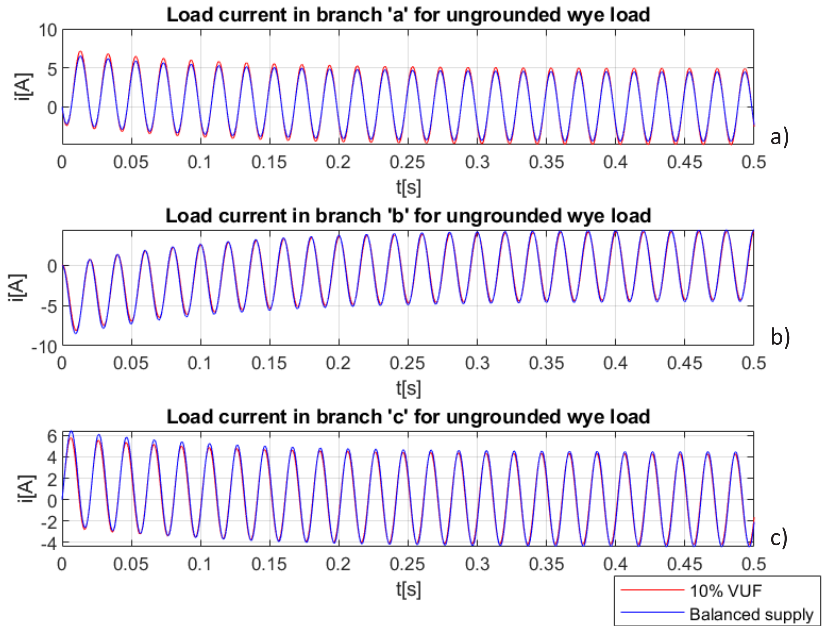

Figure 5: *Load currents over time for an ungrounded wye connected load with balanced power supply and a 10% VUF in a) branch 'a', b) branch 'b', and c) branch 'c' of the load*

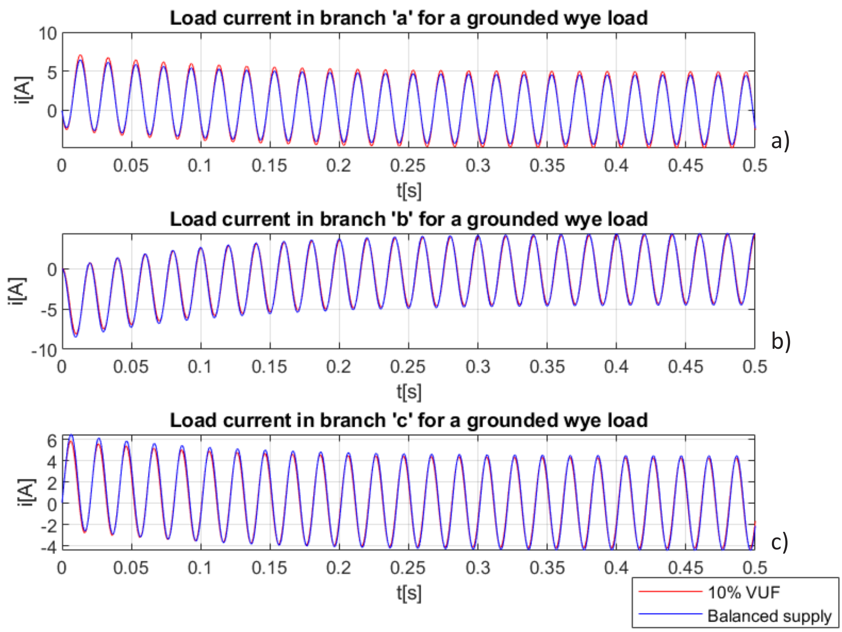

Figure 6: *Load currents over time for a grounded wye connected load with balanced power supply and a 10% VUF in a) branch 'a', b) branch 'b', and c) branch 'c' of the load*

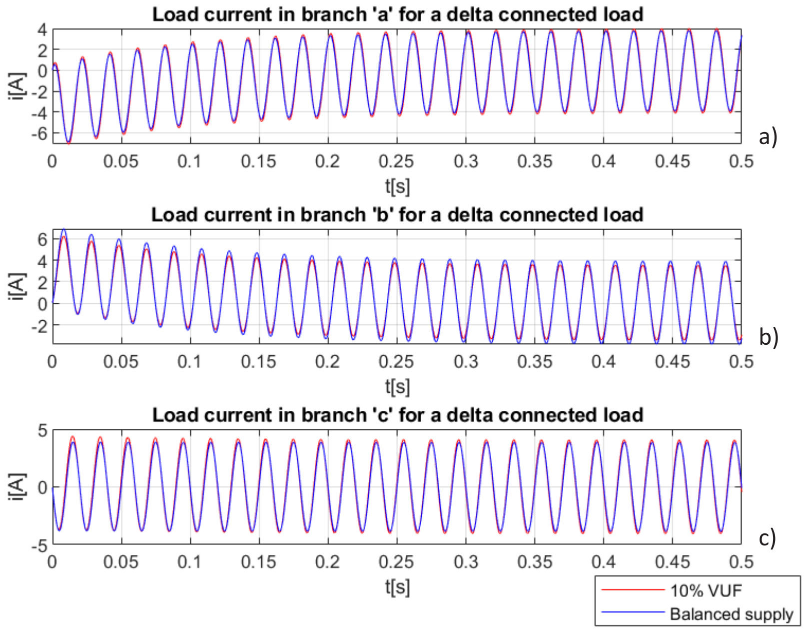

Figure 7: *Load currents over time for a delta connected load with balanced power supply and a 10% VUF in a) branch 'a', b) branch 'b', and c) branch 'c' of the load*

Table 1: *Relative sum* $i^2_{n,sum,rel}$ *for values of VUF between 0 to 10% for an ungrounded wye connected load*

VUF [%] $i^2_{n,sum,rel}$	0	2	4	6	8	10
Subtransient						
Branch 'a'	1.221	1.271	1.321	1.372	1.425	1.478
Branch 'b'	1.925	1.886	1.849	1.812	1.777	1.742
Branch 'c'	1.239	1.201	1.164	1.129	1.096	1.064
Total	4.385	4.358	4.334	4.314	4.297	4.284
Transient						
Branch 'a'	1.010	1.051	1.093	1.135	1.178	1.222
Branch 'b'	1.060	1.039	1.019	0.999	0.981	0.963
Branch 'c'	1.019	0.998	0.978	0.959	0.940	0.923
Total	3.089	3.088	3.089	3.093	3.099	3.108
Quasi-steady-state						
Branch 'a'	1.000	1.040	1.082	1.124	1.166	1.210
Branch 'b'	1.000	0.980	0.962	0.943	0.926	0.910
Branch 'c'	1.000	0.980	0.962	0.944	0.926	0.910
Total	3.000	3.001	3.005	3.011	3.019	3.030

Table 2: *Relative sum* $i^2_{n,sum,rel}$ *for values of VUF between 0 to 10% for a grounded wye connected load*

VUF [%] $i^2_{n,sum,rel}$	**0**	**2**	**4**	**6**	**8**	**10**
Subtransient						
Branch 'a'	1.209	1.258	1.308	1.359	1.411	1.463
Branch 'b'	1.924	1.885	1.847	1.811	1.775	1.740
Branch 'c'	1.252	1.213	1.176	1.141	1.107	1.074
Total	4.385	4.357	4.332	4.310	4.292	4.277
Transient						
Branch 'a'	1.009	1.050	1.092	1.134	1.177	1.221
Branch 'b'	1.060	1.039	1.019	0.999	0.981	0.963
Branch 'c'	1.020	0.999	0.979	0.960	0.941	0.924
Total	3.089	3.088	3.089	3.093	3.099	3.108
Quasi-steady-state						
Branch 'a'	1.000	1.040	1.082	1.124	1.166	1.210
Branch 'b'	1.000	0.980	0.962	0.943	0.926	0.910
Branch 'c'	1.000	0.980	0.962	0.944	0.926	0.910
Total	3.000	3.001	3.005	3.011	3.019	3.030

Table 3: *Relative sum* $i^2_{n,sum,rel}$ *for values of VUF between 0 to 10% for a delta connected load*

VUF [%] $i^2_{n,sum,rel}$	0	2	4	6	8	10
Subtransient						
Branch 'a'	1.667	1.686	1.707	1.728	1.750	1.772
Branch 'b'	1.709	1.641	1.575	1.510	1.446	1.384
Branch 'c'	0.999	1.019	1.040	1.062	1.086	1.111
Total	4.375	4.346	4.321	4.300	4.282	4.268
Transient						
Branch 'a'	1.038	1.058	1.079	1.101	1.123	1.147
Branch 'b'	1.049	1.007	0.966	0.927	0.888	0.849
Branch 'c'	1.000	1.020	1.041	1.063	1.085	1.109
Total	3.087	3.085	3.087	3.090	3.097	3.105
Quasi-steady-state						
Branch 'a'	1.000	1.020	1.042	1.064	1.086	1.110
Branch 'b'	1.000	0.960	0.922	0.884	0.846	0.810
Branch 'c'	1.000	1.020	1.042	1.063	1.086	1.110
Total	3.000	3.001	3.005	3.011	3.019	3.030

As can be seen in Tables 1-3, the relative sum, and with it the Joule losses in the load, increase linearly with the VUF in the quasi-steady-state region of operation. In the cases of a grounded and ungrounded wye connected load, an increase only occurs in branch '*a*', with a factor of about 2, meaning a 10% VUF results in a 20% increase in Joule losses in branch '*a*'. Whilst the Joule losses in the other two branches decrease, there is still a minor net increase in Joule losses in the load. Similarly, in a delta connected load, the Joule losses increase in branches '*a*' and '*c*' in accordance with the VUF, meaning a 10% VUF causes a 10% increase in Joule losses in each branch. The Joule losses in branch '*b*' decrease, however, there is still a minor net increase in Joule losses, as is the case for the wye connected load.

The results are similar in the transient and subtransient region of operation, namely with the wye connected loads there is an increase in Joule losses in branch '*a*' amounting to about twice the VUF, while the losses in the other two phases decrease. Similarly, there is an increase in losses in branches '*a*' and '*c*' in the delta connected load, and a decrease in branch '*b*'. There is minor net increase in Joule losses in all three load connections in the transient region of operation, and a minor decrease in the subtransient region.

These results show that, whilst the total Joule losses in the load increase slightly or even decrease with a higher VUF, the losses in a particular branch increase by a factor of the VUF or twice that, depending on the connection of the load.

The effect of a zero-sequence unbalance on the Joule losses was only observed in the case of a grounded wye connected load. Figure 8 shows the currents in each branch of the load over time for a 10% ZSVUF and balanced power supply. The zero-sequence unbalance in supply voltages does not affect the currents of ungrounded and delta connected loads since there is no path where the zero-sequence current could close.

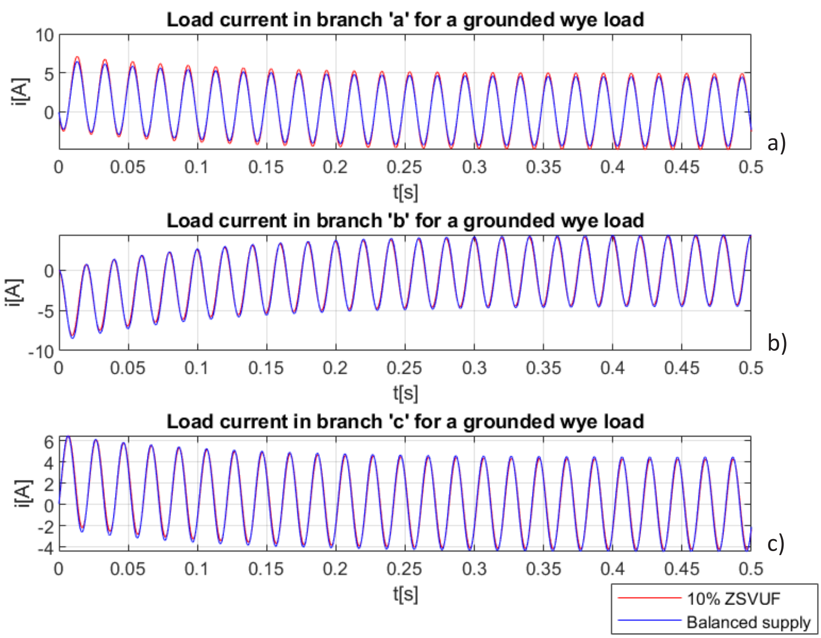

Figure 8: *Load currents over time for a grounded wye connected load with balanced power supply and a 10% ZSVUF in a) branch 'a', b) branch 'b', and c) branch 'c' of the load*

As can be seen in Figure 8, similarly to the negative-sequence voltage unbalance, the zero-sequence voltage unbalance causes an increase in the amplitude of the current in branch '*a*', while the amplitude in branches '*b*' and '*c*' decreases.

The values of $i^2_{n,sum,rel}$ in the subtransient, transient and quasi-steady-region of operation are show in Table 4 for different values of the ZSVUF.

Table 4: *Relative sum* $i^2_{n,sum,rel}$ *for values of ZSVUF between 0 to 10% for a grounded wye connected load*

ZSVUF [%] $i^2_{n,sum,rel}$	**0**	**2**	**4**	**6**	**8**	**10**
Subtransient						
Branch 'a'	1.209	1.258	1.308	1.359	1.411	1.463
Branch 'b'	1.924	1.887	1.851	1.816	1.782	1.748
Branch 'c'	1.252	1.242	1.232	1.224	1.217	1.210
Total	4.385	4.387	4.391	4.399	4.409	4.422
Transient						
Branch 'a'	1.009	1.050	1.092	1.134	1.177	1.221
Branch 'b'	1.060	1.039	1.019	1.001	0.982	0.965
Branch 'c'	1.020	1.001	0.983	0.966	0.949	0.933
Total	3.089	3.091	3.094	3.100	3.109	3.120
Quasi-steady-state						
Branch 'a'	1.000	1.040	1.082	1.124	1.166	1.210
Branch 'b'	1.000	0.980	0.962	0.944	0.927	0.910
Branch 'c'	1.000	0.980	0.962	0.944	0.926	0.910
Total	3.000	3.001	3.005	3.011	3.019	3.030

As can be seen in Table 4, the ZSVUF has the same effect as the VUF, as shown in Table 2, with an increase in Joule losses of twice the ZSVUF in branch '*a*', a decrease in the other two branches and a minor net increase of $i^2_{n,sum,rel}$ in the transient and quasi-steady-state region of operation. However, there is also a minor net increase in losses in the subtransient region.

Furthermore, the effects of a simultaneous negative-sequence and zero-sequence supply voltage unbalance on the currents of a grounded wye connected load were investigated. Figure 9 shows the currents in each branch for the cases of a 10% VUF and ZSVUF and balanced power supply voltages.

Figure 9 shows an increase in the amplitude of the current in branch '*a*' in the case of a voltage unbalance, compared to the case of the balanced voltage supply, and a decrease in the amplitude of the current in the other two branches.

The values of $i^2_{n,sum,rel}$ for different values of simultaneous VUF and ZSVUF are given in Table 5.

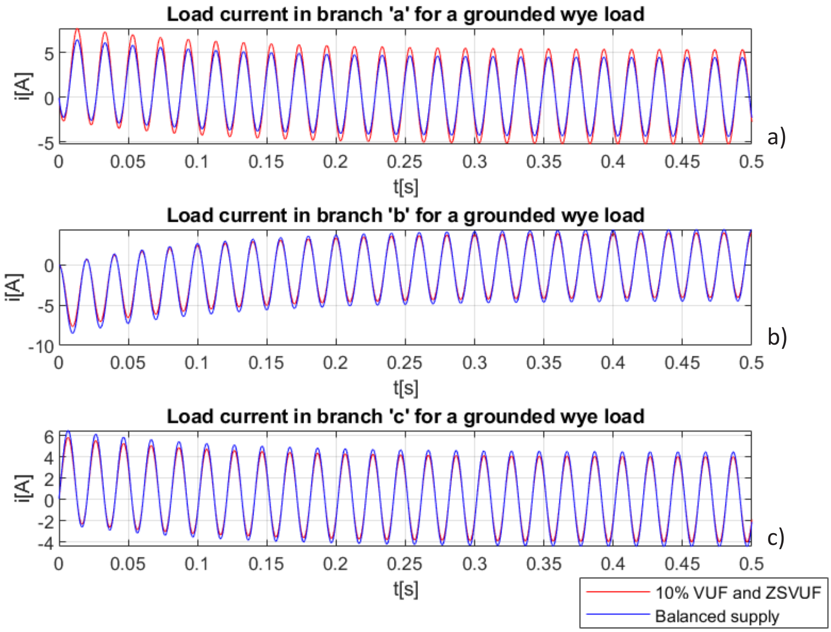

Figure 9: *Load currents over time for a grounded wye connected load with balanced power supply and a simultaneous 10% ZSVUF and VUF in a) branch 'a', b) branch 'b', and c) branch 'c' of the load*

Table 5: *Relative sum $i^2_{n,sum,rel}$ for values of simultaneous ZSVUF and VUF between 0 to 10% for a grounded wye connected load*

VUF and ZSVUF [%] $i^2_{n,sum,rel}$	**0**	**2**	**4**	**6**	**8**	**10**
Subtransient						
Branch 'a'	1.209	1.308	1.411	1.517	1.627	1.741
Branch 'b'	1.924	1.848	1.773	1.700	1.629	1.559
Branch 'c'	1.252	1.202	1.154	1.106	1.060	1.014
Total	4.385	4.358	4.338	4.323	4.315	4.314
Transient						
Branch 'a'	1.009	1.092	1.177	1.266	1.358	1.454
Branch 'b'	1.060	1.018	0.977	0.936	0.897	0.858
Branch 'c'	1.020	0.980	0.940	0.901	0.863	0.826
Total	3.089	3.089	3.094	3.104	3.119	3.138
Quasi-steady-state						
Branch 'a'	1.000	1.082	1.166	1.254	1.346	1.440
Branch 'b'	1.000	0.960	0.922	0.884	0.846	0.810
Branch 'c'	1.000	0.960	0.922	0.884	0.846	0.810
Total	3.000	3.002	3.010	3.022	3.038	3.060

The results shown in Table 5 show that the Joule losses in branch '*a*' increase by four times the value of the simultaneous VUF and ZSVUF. As is the case for the VUF and ZSVUF changing separately, there is a decrease in Joule losses in the other two branches of the load, and like the increase in branch '*a*', it is about double the decrease in the cases with just a VUF or ZSVUF. The minor net increase of losses in the transient and quasi-steady-state region of operation also doubles, and the minor net decrease in the subtransient region is lower than the case of just a VUF, as shown in Table 2. These results suggest the effects of a negative-sequence and zero-sequence supply voltage unbalance are additive.

The results shown in Tables 1 to 5 represent the relative Joule losses over one period. In order to calculate the total relative losses over the 0.5s period shown in Figures 5 to 9, a sum of the $i^2_{n,sum,rel}$ values should be formed, with the subtransient value multiplied by 5, the transient $i^2_{n,sum,rel}$ value multiplied by 15, and the quasi-steady-state $i^2_{n,sum,rel}$ value multiplied by 5, since that is the number of periods in the three discussed regions.

Due to supply voltage unbalances to an iron core inductor load with linear magnetic behaviour, the Joule losses in one branch can increase by the VUF if the load is connected into delta, twice the VUF if the load is connected into ungrounded wye, and twice the sum of the VUF and ZSVUF when the load is connected into grounded wye.

4.2 Effects of supply voltage unbalances on iron core inductor loads with magnetically non-linear behaviour

The simulation was conducted for the loads consisting of iron core inductors with magnetically non-linear behaviour, where variable dynamic inductances were applied to consider the iron core saturation as described in section 3.3. Due to convergence issues, the results for ungrounded wye connected loads are inconclusive and therefore not included in this paper.

Figure 10 shows the load current over time in each branch of the delta connected load for the cases of a balanced power supply, and a 10% VUF, while Figure 11 shows the same results for a grounded wye connected load.

As can be seen in Figures 10 and 11, the currents generally behave similarly to the case with a load with magnetically linear behaviour. Namely, due to the supply voltage unbalance the current amplitude increases in branch '*a*' and decreases in the other two branches for the grounded wye connected load, whilst it increases in branches '*a*' and '*c*', and decreases in branch '*b*' for the delta connected load. However, the decrease in the dynamic inductance due to the saturation, after reaching the saturation value of the current, causes a rapid increase in the current amplitude. This can be observed in the subtransient and partially the transient region of operation for both load connections. Additionally, in the case of the grounded wye connected load, the effects of saturation are also visible in the quasi-steady-state region of operation in branch '*a*', when the VUF is 10%, since the current increase due to the supply voltage unbalance causes the current to reach values above the saturation threshold. This is not the case for the delta connected load, due to the current increase being in both branches '*a*' and '*c*' with a lower value.

To better present the impact of these effects on current responses and thus Joule losses, the relative sums $i^2_{n,sum,rel}$ are given in Table 6 for the delta connected load and in Table 7 for the grounded wye connected load.

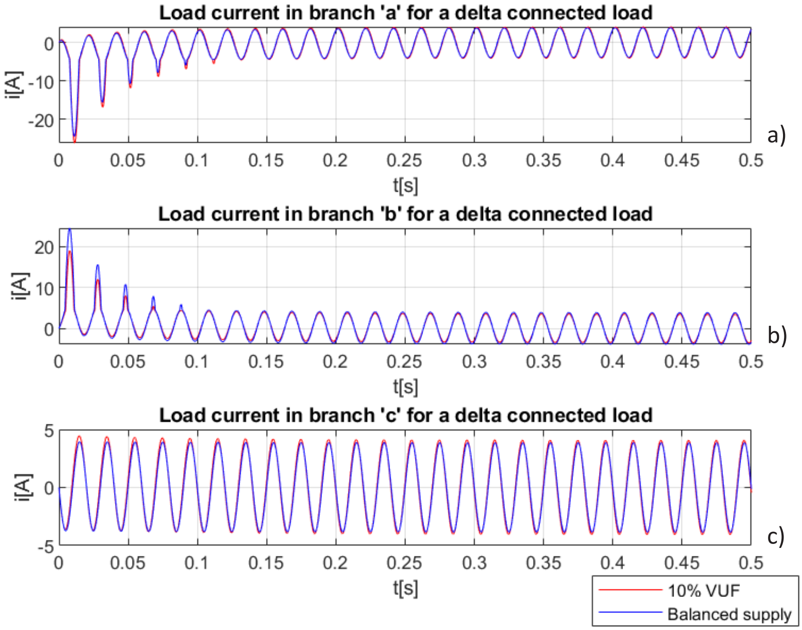

Figure 10: *Load currents over time for a delta connected iron core inductor with magnetically non-linear behaviour with a balanced voltage supply and a 10% VUF in a) branch 'a', b) branch 'b', and c) branch 'c' of the load*

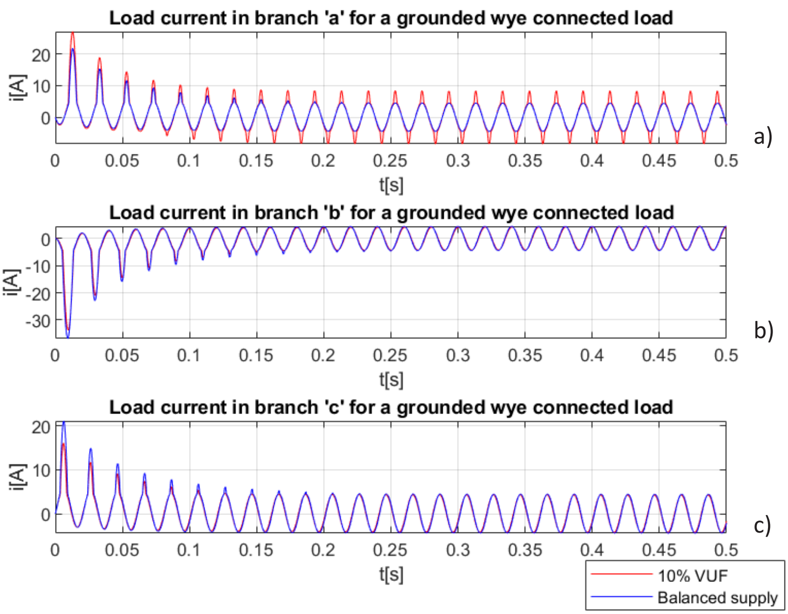

Figure 11: *Load currents over time for a grounded wye connected iron core inductor with magnetically non-linear behaviour with a balanced voltage supply and a 10% VUF in a) branch 'a', b) branch 'b', and c) branch 'c' of the load*

Table 6: *Relative sum $i^2_{n,sum,rel}$ for values of VUF between 0 to 10% for a delta connected iron core inductor load*

VUF [%] $i^2_{n,sum,rel}$	0	2	4	6	8	10
Subtransient						
Branch ‘a’	5.446	5.611	5.777	5.968	6.143	6.344
Branch ‘b’	5.468	4.957	4.481	4.026	3.613	3.222
Branch ‘c’	0.999	1.019	1.040	1.063	1.087	1.113
Total	11.913	11.587	11.298	11.057	10.843	10.679
Transient						
Branch ‘a’	1.010	1.030	1.051	1.073	1.096	1.120
Branch ‘b’	1.015	0.977	0.939	0.903	0.866	0.831
Branch ‘c’	1.000	1.020	1.041	1.063	1.085	1.109
Total	3.025	3.027	3.031	3.038	3.048	3.060
Quasi-steady-state						
Branch ‘a’	1.000	1.020	1.042	1.064	1.086	1.110
Branch ‘b’	1.000	0.960	0.922	0.884	0.847	0.810
Branch ‘c’	1.000	1.020	1.042	1.063	1.086	1.110
Total	3.000	3.001	3.005	3.011	3.019	3.030

Table 7: *Relative sum $i^2_{n,sum,rel}$ for values of VUF between 0 to 10% for a grounded wye connected iron core inductor load*

VUF [%] $i^2_{n,sum,rel}$	0	2	4	6	8	10
Subtransient						
Branch ‘a’	3.504	3.860	4.249	4.667	5.068	5.535
Branch ‘b’	9.951	9.579	9.199	8.855	8.507	8.182
Branch ‘c’	3.387	3.095	2.813	2.553	2.311	2.087
Total	16.843	16.534	16.261	16.075	15.885	15.804
Transient						
Branch ‘a’	1.023	1.087	1.206	1.391	1.636	1.942
Branch ‘b’	1.052	1.024	0.998	0.975	0.954	0.934
Branch ‘c’	1.027	1.001	0.978	0.956	0.936	0.918
Total	3.102	3.112	3.182	3.322	3.526	3.794

VUF [%] $i^2_{n,sum,rel}$	0	2	4	6	8	10
Quasi-steady-state						
Branch 'a'	1.000	1.054	1.188	1.385	1.637	1.943
Branch 'b'	1.000	0.980	0.962	0.944	0.926	0.910
Branch 'c'	1.000	0.980	0.962	0.944	0.927	0.910
Total	3.000	3.014	3.112	3.273	3.490	3.763

The comparison of the results shown in Tables 3 and 6 shows that in the quasi-steady-state region of operation there is no difference between the relative sum $i^2_{n,sum,rel}$ of the delta connected iron core inductors with magnetically linear and non-linear behaviour, due to the currents remaining below the saturation threshold even in the case of unbalanced supply voltages. This is not the case with the grounded wye connected load, as can be seen from Tables 2 and 7. Whilst the decrease in Joule losses ($i^2_{n,sum,rel}$) in branches '*b*' and '*c*' remains equal for the iron core inductors with magnetically linear and non-linear behaviour, the increase in Joule losses in branch '*a*' is not linear but instead approximately proportional to the square of the VUF. This causes the Joule losses to nearly double in the case of a 10% VUF compared to the case of a balanced power supply. This subsequently leads to larger increase in net Joule losses in the load.

The results are similar in the transient region of operation, with the losses in the case of the delta connected load (Table 6) remaining approximately equal to those in Table 3. In the case of a wye connected load, the Joule losses increase proportional to the square of the VUF (Table 7). In the

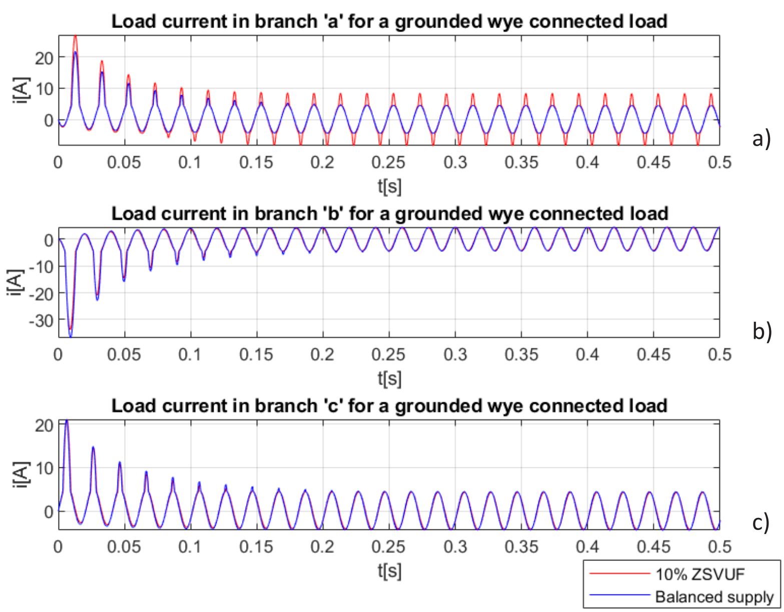

Figure 12: *Load currents over time for a grounded wye connected iron core inductor with magnetically non-linear behaviour with a balanced voltage supply and a 10% ZSVUF in a) branch 'a', b) branch 'b', and c) branch 'c' of the load*

subtransient region, the saturation effects are visible in both loads – the grounded wye and delta connected iron core inductors with magnetically non-linear behaviour (Tables 6 and 7) – due to the currents surpassing the saturation threshold. This causes a larger increase in the Joule losses in branches '*a*' and '*c*' of the delta connected load and in branch '*a*' of the wye connected load. However, these increases are not proportional to the square of the VUF as in the case of the transient or quasi-steady-state region with the wye connected load. Additionally, the relative Joule losses are generally much higher compared to the load with magnetically linear behaviour, even in the balanced case. Even though the total losses increase in general, they decrease with the VUF in a similar way as in the case with a load with magnetically linear behaviour (Tables 2 and 3).

The effects of zero-sequence voltage unbalance can be seen in Figure 12, which shows the load currents over time in a grounded wye connected iron core inductor load with magnetically non-linear behaviour for a 10% ZSVUF and balanced supply voltages.

It is evident from Figure 12 that a zero-sequence voltage unbalance has a similar effect on the current responses as the negative-sequence voltage unbalance seen in Figure 11. The effects of the magnetically non-linear behaviour of the iron core inductor on the relative sum $i^2_{n,sum,rel}$ can be seen in the subtransient and partially transient region of operation in all three branches in the case of the unbalanced and balanced power supply, whilst in quasi-steady-state region it is only present in branch '*a*' in the case of a supply voltage unbalance.

The relative sum $i^2_{n,sum,rel}$ for values of the ZSVUF between 0 and 10% are shown in Table 8.

Table 8: *Relative sum* $i^2_{n,sum,rel}$ *for values of ZSVUF between 0 to 10% for a grounded wye connected iron core inductor load*

ZSVUF [%] $i^2_{n,sum,rel}$	**0**	**2**	**4**	**6**	**8**	**10**
Subtransient						
Branch 'a'	3.504	3.860	4.249	4.667	5.068	5.535
Branch 'b'	9.940	9.572	9.207	8.850	8.527	8.192
Branch 'c'	3.387	3.357	3.328	3.299	3.281	3.272
Total	16.832	16.789	16.784	16.816	16.875	16.998
Transient						
Branch 'a'	1.023	1.087	1.206	1.391	1.636	1.942
Branch 'b'	1.052	1.024	0.999	0.976	0.955	0.935
Branch 'c'	1.027	1.002	0.980	0.960	0.941	0.923
Total	3.102	3.113	3.185	3.326	3.532	3.800
Quasi-steady-state						
Branch 'a'	1.000	1.054	1.188	1.385	1.637	1.943
Branch 'b'	1.000	0.980	0.962	0.944	0.926	0.910
Branch 'c'	1.000	0.980	0.962	0.944	0.927	0.910
Total	3.000	3.014	3.112	3.273	3.491	3.764

Similarly to the effects of the VUF, the ZSVUF causes an increase of $i^2_{n,sum,rel}$, and thus the Joule losses in branch '*a*', which is proportional to the square of the ZSVUF in the transient and quasi-steady-state region of operation. However, the decrease in Joule losses in branches '*b' and 'c' in Table 8 remains the same as in the case with the load with magnetically linear behavio*ur, causing a higher increase in the total Joule losses in these regions than in Table 4. In the subtransient region, a larger increase in total Joule losses is also noticeable, compared to Table 4, however, unlike the values in Table 7, the total losses increase with the ZSVUF, as was in the case with a grounded wye connected load with magnetically linear behaviour (Table 4).

The effects of a simultaneous negative-sequence and positive sequence voltage unbalance are shown in Figure 13, which shows the load currents over time in a grounded wye connected iron core inductor load with magnetically non-linear properties for a simultaneous 10% ZSVUF and VUF and balanced power supply.

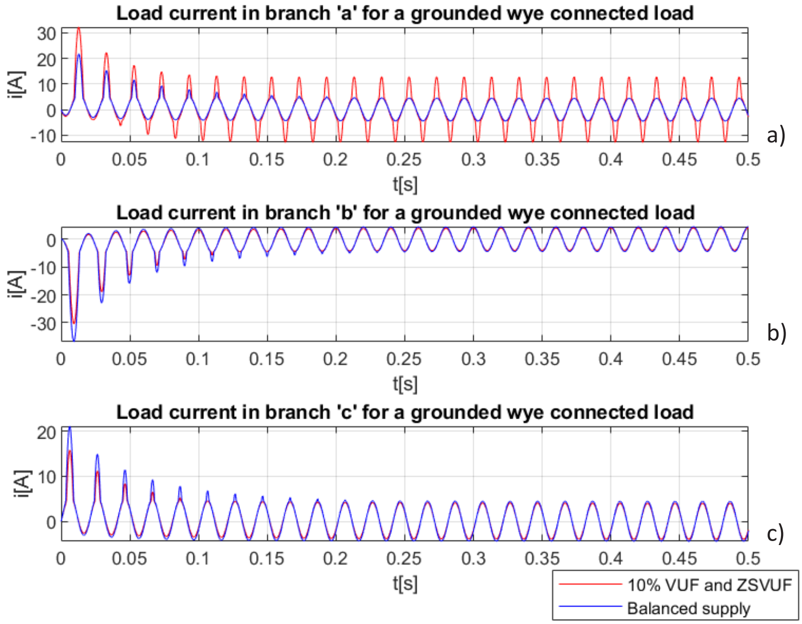

Figure 13: *Load currents over time for a grounded wye connected iron core inductor with magnetically non-linear behaviour with balanced power supply and a simultaneous 10% ZSVUF and VUF in a) branch 'a', b) branch 'b', and c) branch 'c' of the load*

As seen in Figure 13, the amplitude of the current in branch '*a*' increased compared to the cases seen in Figures 11 and 12, however, the overall behaviour remains the same.

Table 9 shows the relative sums $i^2_{n,sum,rel}$ representing the Joule losses.

***Table 9:** Relative sum $i^2_{n,sum,rel}$ for values of simultaneous ZSVUF and VUF between 0 to 10% for a grounded wye connected iron core inductor load*

VUF and ZSVUF [%] $i^2_{n,sum,rel}$	**0**	**2**	**4**	**6**	**8**	**10**
Subtransient						
Branch ‘a’	3.504	4.249	5.068	6.032	7.191	8.533
Branch ‘b’	9.951	9.186	8.462	7.770	7.102	6.483
Branch ‘c’	3.387	3.051	2.736	2.444	2.176	1.920
Total	16.843	16.486	16.265	16.246	16.469	16.936
Transient						
Branch ‘a’	1.023	1.206	1.636	2.306	3.215	4.353
Branch ‘b’	1.052	0.996	0.949	0.904	0.862	0.823
Branch ‘c’	1.027	0.978	0.933	0.892	0.854	0.818
Total	3.102	3.180	3.518	4.102	4.932	5.994
Quasi-steady-state						
Branch ‘a’	1.000	1.188	1.637	2.311	3.226	4.361
Branch ‘b’	1.000	0.960	0.922	0.884	0.846	0.810
Branch ‘c’	1.000	0.961	0.922	0.884	0.847	0.810
Total	3.000	3.109	3.481	4.078	4.919	5.982

The results shown in Table 9 indicate that the simultaneous negative-sequence and zero-sequence voltage unbalances result in an increase in Joule losses in branch ‘a’ of the load, which is proportional to approximately double the square value of the VUF and ZSVUF in the transient and quasi-steady-state region. In the case of a 10% simultaneous VUF and ZSVUF this means more than four times the Joule losses in that branch than in the case of a balanced power supply. Furthermore, due to the losses not increasing in other branches compared to the case with a load with magnetically linear behaviour (Table 5), compared to the case with a balanced power supply, the total losses almost doubled as well. In the subtransient region, the Joule losses in branch ‘a’ also increased compared to Table 5, although not proportional to the square value of the VUF and ZSVUF. At a 10% zero-sequence and negative-sequence voltage unbalance, the losses in branch ‘a’ are more than double those in the case of a balanced power supply. Additionally, due to the larger increase in losses caused by the zero-sequence voltage unbalance, the total Joule losses slightly increased with the VUF and ZSVUF. These results suggest that the effects of the VUF and ZSVUF are additive in the case of an iron core inductor load with magnetically non-linear behaviour.

The results show that due to supply voltage unbalances of an iron core inductor load with magnetically linear behaviour, the Joule losses in one branch, compared to the case of a balanced power supply, can increase by the VUF if the load is connected into delta, and twice the sum of the square values of the VUF and ZSVUF when the load is connected into grounded wye. This means that in a grounded wye connected load with magnetically non-linear behaviour, even small supply voltage unbalances can lead to a larger loss of efficiency and overheating.

5 CONCLUSION

This work proposes a unified method for evaluating the impact of supply voltage unbalances on the increase in currents and Joule losses of wye and delta connected loads. It considers the magnetically linear or non-linear behaviour of iron core conductors in subtransient, transient and quasi-steady-state operation. The supply voltage unbalances are characterised by the VUF and ZSVUF. The proposed method is based on Dommel's method, which utilises a modified nodal potential method, implicit numerical integration and time discretisation for dynamic and quasi-steady-state simulations of electric circuits. The magnetically non-linear behaviour of iron core indictors is considered in the form of variable current dependent dynamic inductances.

Although the proposed method is demonstrated in the case studies of wye and delta connected loads consisting of iron core inductors with magnetically linear and non-linear behaviour, it can be extended towards applicability to electrical machines. The results presented in the paper clearly show to what extent the supply voltage unbalances influence the currents in the branches and corresponding Joule losses of the discussed loads in subtransient, transient and quasi-steady-state operation.

References

[1] **A. von Jouanne, B. Banerjee:** *Assessment of voltage unbalance,* IEEE Transactions on Power Delivery, vol.16, no. 4 pp.782-790, 2001

[2] **IEEE STANDARDS ASSOCIATION:** *IEEE Recommended Practice for Monitoring Electric Power Quality*, IEEE, p.p.25-28, 2019, DOI: 10.1109/IEEESTD.2019.8796486

[3] **Y. Wang:** *Analysis of effects of three-phase voltage unbalance on induction motors with emphasis on the angle of the complex voltage unbalance factor*, IEEE Transactions on Energy Conversion, vol.16, no.3, p.p.270-275, 2001

[4] **Y. Wang:** *An analytical study on steady-state performance of an induction motor connected to unbalanced three-phase voltage*, 2000 IEEE Power Engineering Society Winter Meeting. Conference Proceedings, p.p.159 – 164, 2000

[5] **J. Faiz, H. Ebrahimpour, P. Pillay:** *Influence of unbalanced voltage on the steady-state performance of a three-phase squirrel-cage induction motor*, IEEE Transactions on Energy Conversion, vol.19, no.4, pp.657-662, 2004

[6] **C. T. Raj, P. Agarwal, S. P. Srivastava:** *Performance Analysis of a Three-Phase Squirrel-Cage Induction Motor under Unbalanced Sinusoidal and Balanced Non-Sinusoidal Supply Voltages*, 2006 International Conference on Power Electronic, Drives and Energy Systems, p.p.1-4, 2006

[7] **J. Faiz, H. Ebrahimpour:** *Precise derating of three-phase induction motors with unbalanced voltages*, Fourtieth IAS Annual Meeting. Conference Record of the 2005 Industry Applications Conference, p.p.485-491, 2005

[8] **E. C. Quispe, I. D. Lopez:** *Effects of unbalanced voltages on the energy performance of three-phase induction motors*, 2015 IEEE Workshop on Power Electronics and Power Quality Applications (PEPQA), p.p.1-6, 2015

[9] **K. Lee, G. Venkataramanan, T. M. Jahns:** *Modeling Effects of Voltage Unbalances in Industrial Distribution Systems With Adjustable-Speed Drives*, IEEE Transactions on Industry Applications, vol.44, no.5, p.p.1,322-1,332, 2008

[10] **P. Gnacinski:** *Windings Temperature and Loss of Life of an Induction Machine Under Voltage Unbalance Combined With Over- or Undervoltages*, IEEE Transactions on Energy Conversion, vol.23, no.2, p.p.363-371, 2008

[11] **J. L. Gonzalez-Cordoba, R. A. Osornio-Rios, D. Granados-Lieberman, R. D. J. Romero-Troncoso, M. Valtierra-Rodriguez:** *Correlation Model Between Voltage Unbalance and Mechanical Overload Based on Thermal Effect at the Induction Motor Stator*, IEEE Transactions on Energy Conversion, vol.32, no.4, pp.1,602-1,610, 2017

[12] **P. Sudasinghe, U. Jayatunga, P. Commins, J. Moscrop, S. Perera:** *Dependancy of Three Phase Induction Motor Derating Aspects on Complex Voltage Unbalance Factor: A Calorimetric and Finite Element Simulation Study*, IEEE Access, vol.9, p.p.147,063-147,071, 2021

[13] **G. Štumberger, B. Štumberger, T. Maričič:** *Magnetically nonlinear dynamic models of synchronous machines and experimental methods for determining their parameters*, Energies, vol.12, no.18, p.p.1-22, 2019

[14] **J. Arrillaga,** *Computer modelling of electrical power systems*, Wiley, 2001

[15] **G. Štumberger, Ž. Plantić, B. Štumberger, T. Maričič:** *Impact of static and dynamic inductance on calculated time response*, Przeglęad Elektrotechniczny, vol.87, iss. 3, p.p.190-193, 2011

Nomenclature

(Symbols)	(Symbol meaning)
$\underline{V}_0$	Phasor of the zero-sequence voltage
$\underline{V}_1$	Phasor of the positive-sequence voltage
$\underline{V}_2$	Phasor of the negative-sequence voltage
$\underline{V}_a$	Phasor of the voltage phase voltage in phase 'a'
$\underline{V}_b$	Phasor of the voltage phase voltage in phase 'b'
$\underline{V}_c$	Phasor of the voltage phase voltage in phase 'c'
exp	Exponential function
a	$\exp\left(j2\frac{\pi}{3}\right)$

Nomenclature

(Symbols)	(Symbol meaning)
j	Imaginary unit
VUF	Voltage unbalance factor
ZSVUF	Zero sequence voltage unbalance factor
$u_L(t)$	Inductor voltage
$v_k(t)$	Potential in point k
$v_m(t)$	Potential in point m
$i_{km}(t)$	Inductor current at time t
L	Inductance
t	Time
Δt	Time period
	Auxiliary variable
$f\left(x\left(t\right),t\right)$	Integrated function
$x\left(t\right)$	Value of the integral of function f
$I_{km}\left(t\text{-}\Delta t\right)$	Current describing the history of the inductor current
$i_n\left(t\right)$	Current of a phase
$u_n\left(t\right)$	Supply voltage of a phase
n	Index denoting one of the phases, $n \quad \left\{a,b,c\right\}$
R	Resistance of the current source and cable
$\underline{V}_n$	Phasor of the supply voltage of phase *n*
L_n	Inductance of the iron core inductor in branch *n*
R_L	Load resistance
I	Current vector
G	Impedance matrix
G’	The inverse of the impedance matrix
V	Node potential vector
$i_{L_n}(t)$	Load current in branch *n*
$i^2_{n,sum}$	The sum of the squared instantaneous value of the load current in branch *n*

Nomenclature

(Symbols)	(Symbol meaning)
t_{start}	Start time of a region of operation
t_{stop}	Stop time of a region of operation
$i^2_{n,sum,rel}$	Sum of the squared instantaneous values of the load current in branch *n* normalised over one period
N	Number of periods
$i^2_{n,sum,0}$	The sum of the squared instantaneous value of the load current in branch *n* during a balanced power supply and quasi-steady-state region of operation
Ψ	Flux linkage
L_{dn}	Dynamic inductance of the load in branch *n*